Research Article

CT-Based Ocular Biometry and Three-Dimensional Printing of the Domestic Donkey Eye

Meray Nabil Ramsis[1], Ayman Tolba Reyad[1], Yara Sayed Abouelela[1], Mohammed Ali Albahrawy[2]

[1]Anatomy and Embryology Department, Faculty of Veterinary Medicine, Cairo University, Giza, Egypt; [2]Department of Surgery, Anesthesiology and Radiology, Faculty of Veterinary Medicine, Mansoura University, Egypt.

Abstract | Accurate anatomical data of ocular structures are essential for diagnosing ophthalmic diseases and guiding surgical interventions in veterinary medicine. This study aimed to provide baseline CT-based biometric reference values for the ocular globes of clinically normal domestic donkeys and to evaluate the use of 3D scanning and printing for creating anatomical models. A total of ten adult donkeys were included in the study. Eight donkeys underwent *in vivo* CT imaging, and both eyes from each animal were used for biometric measurements, resulting in 16 eyes for assessment of axial globe length, posterior wall thickness, central lens thickness, and Latero-medial distances of the globe and lens. Additionally, four isolated eyeballs were scanned and 3D-printed using polylactic acid (PLA) to create magnified anatomical models for detailed morphological examination. The donkey eyeball was predominantly spheroidal, with morphometric analysis showing no significant differences between right and left eye ($P > 0.05$). Key biometric measurements included a mean axial length of 36.78 ± 3.23 mm (right) and 36.46 ± 3.22 mm (left; $p = 0.864$), a central lens diameter of 9.32 ± 0.44 mm (right) and 9.94 ± 0.52 mm (left; $p = 0.051$), and a latero-medial lens diameter of 15.67 ± 0.56 mm (right) and 15.79 ± 0.55 mm (left; $p = 0.713$). These data provide immediate access to the main biometric findings and confirm the absence of significant interocular differences. The 3D-printed models visually resembled the scanned anatomy and represent a practical, reusable, and ethically responsible alternative to cadaveric specimens for teaching and surgical training. Although no quantitative dimensional validation was performed, qualitative comparison with CT images indicated accurate representation of the overall anatomical features. These results provide reliable CT reference data for donkey ophthalmology and highlight the potential of 3D modeling to support veterinary anatomical education while adhering to modern animal welfare standards. Further studies are needed to assess their educational effectiveness and impact on surgical skill acquisition.

Keywords | Anatomy dimensions, Computed tomography, Donkey, Eye, 3D printing models, 3D scanning

Received | February 13, 2026; **Accepted** | February 27, 2026; **Published** | May 11, 2026
***Correspondence** | Meray Nabil, Anatomy and Embryology Department, Faculty of Veterinary Medicine, Cairo University, Giza, Egypt; **Email:** meraynabil122@gmail.com
Citation | Ramsis MN, Tolba A, Abouelela YS, Albahrawy MA (2026). CT-Based ocular biometry and three-dimensional printing of the domestic donkey eye. Adv. Anim. Vet. Sci., 14(5):996-1004.
DOI | https://dx.doi.org/10.17582/journal.aavs/2026/14.5.996.1004
ISSN (Online) | 2307-8316

INTRODUCTION

The domestic donkey (*Equus asinus*) is a globally significant species, represented by approximately 107 million animals worldwide (Burden and Bell, 2019). Historically valued for transportation and labor (Monti *et al*., 2007), donkeys continue to play important economic roles in both developing and developed countries, contributing through milk production (Salimei and Fantuz, 2012), meat in markets such as China and Russia, and high-demand skin products (Burden and Bell, 2019). The productivity and utility of donkeys depend on their

overall health, including adequate vision function, as ocular diseases can impair feeding, mobility, and reproductive performance. Such impairments can negatively affect both animal welfare and economic value. Therefore, a detailed understanding of donkey ocular anatomy is necessary to support accurate diagnosis, effective management, and prevention of vision-related disorders. Comprehensive anatomical reference data is essential for clinicians and researchers to appropriately diagnose and manage ophthalmic conditions (Carastro, 2005; Misk, 1990).

Although equine reference data largely derived from horses are commonly applied in clinical practice, donkeys (*Equus asinus*) exhibit species-specific anatomical differences that limit the direct applicability of horse-based values. Notably, donkeys demonstrate distinct ocular biometry, including a smaller globe size and variations in internal ocular structures, which may influence diagnostic interpretation and surgical planning (Attaai *et al*., 2022).

Donkeys are affected by a range of ophthalmic disorders, including corneal ulcers, cataracts, uveitis, lens luxation, ocular tumors, and nasolacrimal obstructions (Laus et al., 2024; Mendoza *et al*., 2018; Misk, 1990), with relatively high prevalence reported in certain populations. Precise ocular measurements, such as posterior wall thickness, axial length, lens diameter, and chamber dimensions, are particularly relevant for these conditions, as small variations in ocular biometry can influence surgical planning, intraocular device placement, and prognosis. For instance, a posterior wall thickness of 2.03 mm serves as a baseline reference; deviations potentially indicating pathological changes such as edema, inflammation, tumors, or atrophy. These anatomical and clinical considerations highlight the necessity of donkey-specific ocular reference data to ensure accurate diagnosis, guide surgical interventions, and minimize errors that could result from applying generalized equine values.

The donkey eyeball is structured into three distinct layers: the fibrous outer layer (cornea and sclera), the vascular middle layer (uvea, including the choroid, ciliary body, and iris), and the inner nervous layer (retina) (Bloom and Fawcett, 1970; Davson, 1963; Gelatt, 2013; Samuelson, 1999; Singh *et al*., 2017). Precisely identifying the integrity of these orbital structures is paramount when planning surgical strategies (Lakits *et al*., 1999).

Computed Tomography (CT) is a superior imaging modality for evaluating ocular structures due to its high-resolution, cross-sectional capabilities, which facilitate detection of foreign bodies, trauma, and subtle anatomical variations, even when clinical examination is limited (Bagaria and Chaudhary, 2017; Finkelstein *et al*., 1997; Grove, 1982). Despite these advantages, standardized ocular CT reference values for donkeys (*Equus asinus*) are lacking, likely due to technical and logistical challenges, precise positioning requirements, and limited access to veterinary CT facilities for large animals. In this study, we overcame these obstacles using optimized *in-vivo* scanning protocols and supplementary by *ex-vivo* scans. *In vivo* measurements provided physiologically accurate reference values, while *ex vivo* data offered detailed anatomical insights and supported 3D model development, together enabling comprehensive, species-specific ocular reference data for donkeys.

Beyond diagnostics, there is a growing need for innovative educational tools in veterinary medicine. The complexity of the donkey eyeball can be better visualized through 3D modeling, which has the potential to enhance learning experiences for students and provide a safe, ethical environment for residents to practice surgical procedures (Singh and Sahu, 2023). Although this study did not directly assess the impact of 3D models on learning outcomes or surgical skill acquisition, it aims to fill the current knowledge gap by establishing CT-scan biometric reference values for clinically normal donkeys, assessing interocular (laterality) differences, and developing a 3D-printed anatomical model as a high-fidelity alternative to cadaveric specimens for veterinary training. Future studies are needed to quantitatively evaluate the educational benefits of these models.

MATERIALS AND METHODS

Ethical approval

All procedures involving animals were approved by the Veterinary Medicine Cairo University Institutional Animal Care and Use Committee (Approval No. Vet-CU.110520251110). The study adhered to internationally recognized guidelines for the care and use of animals in research. Ethical considerations included minimizing the use of live animals and substituting cadaveric specimens and 3D models wherever possible to comply with the "3Rs" principle (Replacement, Reduction, Refinement).

Animals and specimens

Ten clinically healthy adult male donkeys (*Equus asinus*), aged 4–7 years, were included in this study. All animals underwent complete ophthalmic examinations prior to imaging to exclude pre-existing ocular abnormalities. For *in vivo* CT imaging, eight live donkeys were scanned, providing a total of sixteen eyes for biometric measurements. In addition, two cadaveric donkeys obtained from the dissecting laboratory of the Department of Anatomy were used for ex-vivo investigations, contributing four additional eyes. Thus, a total of twenty eyes (sixteen *in vivo* and four *ex-vivo*) were included in the biometric analysis (Table 3).

For gross anatomical evaluation of the tapetum lucidum and internal ocular structures, careful corneal incisions were performed to expose the lens, vitreous body, and inner choroidal surface. All procedures involving live animals and post-mortem specimens were conducted in accordance with institutional animal care and used guidelines to preserve anatomical integrity and minimize distress. Ethical approval for the study was obtained from the appropriate institutional review board.

Computed tomography (CT) imaging and biometry

CT examinations were performed on eight live donkeys (sixteen eyes) using a 16-slice multi-detector CT scanner (50 cm field of view, 512 × 512 matrix, 1.25 mm slice thickness, 1.25 mm interslice gap). Scanning parameters were standardized at 120 kV and 200 mA to ensure optimal image resolution while minimizing radiation exposure. To prevent motion artifacts, animals were sedated using a standardized protocol consisting of intravenous xylazine (1.1 mg/kg) and positioned in sternal recumbency with the head symmetrically extended and supported to maintain alignment of the skull. The head was secured to avoid rotation or tilt, ensuring consistent anatomical orientation across all subjects. Multiplanar reconstructions were generated in parasagittal and transverse planes to visualize the globe's maximum dimensions. All biometric measurements were performed by a single experienced veterinary radiologist to reduce inter-observer variability. Each parameter was measured three times on separate occasions, and the mean value was used for statistical analysis.

The following ocular biometric parameters were recorded for each eye:

- Axial Length (AL): Maximum anteroposterior distance from the central cornea to the retina.
- Anterior Chamber Depth (ACD): Anteroposterior distance from the corneal endothelium to the anterior lens capsule, measured perpendicular to the corneal plane.
- Maximum Latero-medial Globe Distance (LMG): Maximum equatorial width perpendicular to the axial length.
- Posterior Chamber Depth (PCD): Distance from the posterior lens capsule to the retina.
- Central Lens Diameter (CLD): Maximum anteroposterior thickness of the lens.
- Latero-medial Lens Distance (LML): Maximum horizontal lens width.
- Posterior Wall Thickness (PWT): Thickness of the combined retinochoroidal-scleral complex.
- Eyes with imaging artifacts, evidence of ocular, retrobulbar, or sinus pathology, or poor image quality were excluded from analysis.

3D modeling and printing

Four isolated donkey eyes were scanned using a handheld 3D scanner (EinScan Pro 2X, Shining 3D) to generate high-resolution surface data. The scans were processed in Kiri Eng® software to correct errors and smooth surfaces and refined in PrusaSlicer 2.6.2 for slicing and G-code export. Physical replicas were printed using a Prusa i3 MK3S+ 3D printer with PLA filament under controlled parameters (Table 1), and anatomical structures were painted with acrylics to enhance visualization. Models were documented with digital photography and labeled using Adobe Photoshop, with terminology aligned to the (International Committee on Veterinary Gross Anatomical Nomenclature, 2017; Schaller and Constantinescu, 2007). We recognize that no quantitative validation of the printed models dimensions relative to the source eyes was performed. The 3D-printed models were therefore intended primarily as qualitative educational and demonstrative tools to visualize ocular anatomy based on CT-derived measurements, rather than as validated surgical

Table 1: Software and 3D printer parameters for donkey eyeball models.

Parameter category	Parameter	Value	Notes/Clarification
Software settings	Support placement	Everywhere	—
	Support pattern spacing	4 mm	Distance between support structures
	Infill density	70%	—
	Top interface layer of support	Heavy	—
	Support style	Snug	—
	Layer height (for slicing/accuracy)	0.15 mm	Not nozzle diameter; defines print resolution
Printer settings	Printing temperature	215 °C	—
	Nozzle diameter	0.4 mm	Physical hardware of the printer
	Printing time	32 h	—
	Bed type	Smooth glass	Smooth build plate material specified
	Filament material	PLA (polylactic acid)	—
	Filament amount	800 g	—
	Estimated cost	2000 EGP	Filament only excludes labor and equipment depreciation

or biomechanical models. Future studies should incorporate formal dimensional validation using digital caliper measurements or CT re-scanning to confirm accuracy.

Statistical analysis

All ocular biometric data were analyzed using GraphPad Prism 8.4.3 (CA, USA). The normality of each variable was assessed using the Shapiro-Wilk test, and all parameters were confirmed to be normally distributed ($p > 0.05$). Comparisons between the right and left eye of the same donkey were performed using paired Student's T-tests, as the measurements represent matched paired rather than independent observations.

To control the risk of type I error from multiple comparisons (seven parameters), a Bonferroni correction was applied, adjusting the significance threshold to $\alpha = 0.05/7 \approx 0.007$.

All measurements were performed by a single experienced veterinary radiologist trained in ocular imaging and morphometric analysis. The observer was blinded to eye laterality, and to assess repeatability, each parameter was measured three times on separate occasions, with the mean value used for analysis.

Although a formal power analysis was not conducted due to the exploration nature of the study and the limited animal availability, the sample size (n = 10 donkeys) was consistent with previously published studies of ocular biometry in donkeys and other equids (Wafy *et al.*, 2021). Donkeys aged 4–7 years were selected to capture clinically mature adults while minimizing potential confounding effects from juvenile growth or age-related changes, as ocular dimensions can vary with age in equids (Wafy *et al.*, 2021). Data are presented as mean ± SD with 95% confidence intervals (CI). Statistical significance was defined as $p < 0.05$, with adjustments for multiple comparisons applied where appropriate.

RESULTS

Anatomy

In the present study, the ocular globes of all twenty eyes examined from ten clinically healthy adult male donkeys (*Equus asinus*; 4–7 years) were relatively large and globular. The cornea appeared broad and circular in all eyes. The pupils consistently exhibited a horizontal, elliptical shape. Examination of the dorsal fundus revealed a distinct, iridescent tapetum lucidum in all eyes, although minor individual variations in size and reflectivity were noted. Gross inspection of the third eyelid demonstrated a thin, triangular conjunctival fold at the medial canthus in all specimens, internally supported by cartilage and covered by palpebral and bulbar conjunctiva. Pigmentation along the anterior surface and free edge of the third eyelid was present in 18 of 20 eyes, with slight differences in extent and intensity (Figure 2). Both *in vivo* (n= 16) and ex vivo (n= 4) examinations showed consistent anatomical features, supporting the reproducibility of these findings across live and post-mortem specimens.

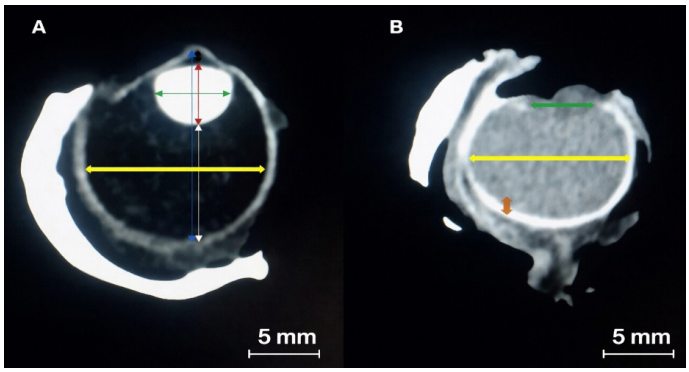

Figure 1: CT-based illustration of donkey ocular biometric measurements. Colored double-headed arrows indicate the measured parameters. (A) Maximum axial length (MAL, blue), anterior chamber depth (ACD, black), latero-medial globe diameter (LMG, yellow), posterior chamber depth (PCD, white), central lens diameter (CDL, red), and latero-medial lens diameter (LML, green). (B) Posterior wall thickness (PWT, brown).

Figure 2: Anatomy of the eyeball.
Muscles: (a) Levator palpebrae superioris, (b) Malaris muscle. Eyeball structures: (1) Cornea, (2) Upper eyelid, (3) Lower eyelid, (4) Third eyelid, (5) Sclera, (6) Corneo-scleral junction, (7) Conjunctiva, (8) Iris, (9) Choroid, (10) Retina, (11) Optic disc (optic papilla), (12) Optic nerve, (13) Suspensory ligament (zonular fibers) of ciliary body, (14) Medial canthus, (15) Lateral canthus, (16) Tapetum of choroid.

A three-dimensional digital reconstruction of the donkey eyeball was generated from CT-derived surface data using volumetric modeling techniques. The reconstruction enabled multi-axial visualization of major ocular structures and allowed spatial assessment of anatomical relationships (Figure 3). The printed model reproduced the general

morphology of the ocular globe and associated structures. Table 2 provides a qualitative comparison between the anatomical specimens and the 3D-printed model, outlining observable structural correspondences and practical differences. No statistical comparisons were performed, as the model was developed for morphological visualization rather than quantitative morphometric validation. The 3D reconstruction was used to complement the anatomical and imaging findings and to enhance structural interpretation without contributing to the biometric reference values reported in this study (Figure 3 and Table 2).

Figure 3: 3D-printed cross-section of the eyeball with extraocular muscles in 100mm. Scale bar and orientation preserved to illustrate dorsal (D), ventral (V), medial (M), lateral (L), Rostral (R) directions.
(1) Cornea, (5) Sclera, (6) Corneo-scleral junction, (9) Choroid, (10) Retina, (12) Optic nerve, (13) Suspensory ligament (zonular fiber), (16) Tapetum of choroid, (17) Anterior chamber, (18) Posterior chamber, (19) Central Retinal artery and vein, (20) Lacrimal gland. Extraocular muscles: (DR) Dorsal Rectus Muscle, (VR) Ventral Rectus Muscle, (VO) Ventral oblique Muscle, (LR) Lateral Rectus Muscle, (RO) Retractor Oculi Muscle, (MR) Medial Rectus muscle, (SO) Superior oblique Muscle.

Computed tomography (CT)

CT imaging of enucleated eyes from clinically normal donkeys enabled clear visualization of the cornea, anterior chamber, uveal tract, lens, vitreous body, optic nerve, and extraocular muscles (Figure 4). The anatomical boundaries of these structures were well delineated on transverse images, allowing consistent morphometric assessment.

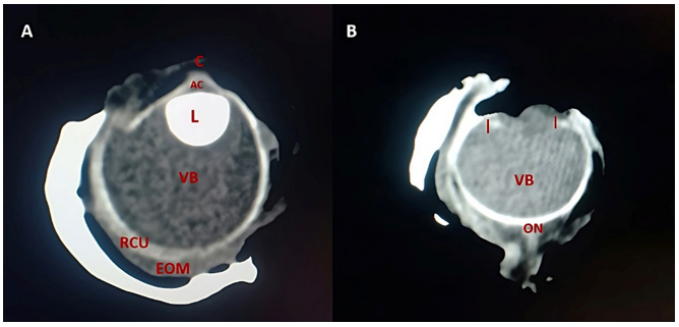

Figure 4: CT scan of a donkey eyeball (axial plane). C, cornea; AC, anterior chamber; L, lens; VB, vitreous body; I, iris; ON, optic nerve; RCU, retinochoroid unit; EOM, Extraocular muscles. Scale bar = 5 mm. Image corresponds to the left eye of donkey.

Anterior segment

The cornea appeared as a hyperdense ring at the anterior pole, whereas the anterior chamber was hypodense due to the presence of aqueous humor.

Uveal tract and lens

The iris and ciliary body formed a moderately dense circumferential structure surrounding the lens. The lens appeared as a well-defined hyperdense structure.

Posterior segment

The vitreous body appeared uniformly hypodense.

Table 2: Practical comparison between real ocular specimens and 3D-printed eye models.

Parameter	Real ocular specimen	3D-printed eye model	Notes
Preservation requirements	Requires refrigeration or chemical preservation; limited shelf life	Stable at room temperature; long-term storage possible	No preservatives needed for 3D models
Handling and manipulation	Fragile soft tissue; may deform or tear with repeated handling	Structurally stable; maintains shape under repeated handling	Observed during lab manipulation
Tissue texture	Native soft tissue texture present	Rigid polymer; tactile properties differ from tissue	Qualitative observation
Ethical considerations	Requires multiple animal specimens for repeated training	One specimen can generate multiple models; reduces need for additional animals	Net reduction in animal use documented
Cost efficiency	Recurring costs for specimen acquisition, preservation, and disposal	Initial printing cost; reusable with minimal maintenance	Observed over study period
Safety and sanitation	Formalin or biological tissue handling requires safety precautions	No chemical preservatives; safe for repeated classroom handling	Reduces exposure to chemicals

Table 3: CT-based ocular measurements of right and left eyes in clinically normal mature donkeys (n = 8, 16 eyes).

Parameter (mm)	Left Eye Mean ± SD	Range (min–max)	95% CI	Right Eye Mean ± SD	Range (min–max)	95% CI	p-value (paired t-test)
Maximum axial length (MAL)	36.46 ± 3.22	33.1–40.2	34.15–38.77	36.78 ± 3.23	33.4–40.5	34.47–39.09	0.864
Anterior chamber depth (ACD)	3.25 ± 0.39	2.8–3.7	2.84–3.66	3.18 ± 0.38	2.8–3.6	2.78–3.58	0.782
Latero-medial globe diameter (LMG)	36.98 ± 1.78	35.0–39.0	35.11–38.86	37.02 ± 1.80	35.2–39.0	35.15–38.89	0.970
Posterior chamber depth (PCD)	16.03 ± 0.72	15.1–17.0	15.27–16.79	15.86 ± 0.73	15.1–16.8	15.10–16.63	0.700
Central lens diameter (CDL)	9.94 ± 0.52	9.1–10.8	9.40–10.48	9.32 ± 0.44	8.8–9.9	8.86–9.78	0.051
Latero-medial lens diameter (LML)	15.79 ± 0.55	15.0–16.6	15.21–16.37	15.67 ± 0.56	15.1–16.4	15.08–16.25	0.713
Posterior wall thickness (PWT)	1.98 ± 0.21	1.7–2.3	1.75–2.20	2.03 ± 0.21	1.8–2.3	1.80–2.25	0.672

MAL, maximum axial length; ACD, anterior chamber depth; LMG, Latero-medial distance of the globe; PCD, posterior chamber depth; CDL, central diameter of lens; LML, Latero-medial diameter of lens; PWT, posterior wall thickness; SD, standard deviation; CI, confidence interval.

Posterior structures and orbit

The optic nerve was visualized as a funnel-shaped hypodense structure. The retina, choroid, and sclera were not clearly separable and were therefore collectively described as the retino-choroid unit. Extraocular muscles were identifiable but demonstrated lower definition compared to the bony orbital structures.

Ocular biometry

Biometric measurements indicated that the donkey ocular globe is predominantly spheroidal. CT-based ocular biometric measurements were compared between the right and left eye using a paired Student's t-test. The measurements were as follows: maximum axial length (MAL: 36.78 ± 3.23 mm vs 36.46 ± 3.22 mm; 95% CI: 34.47–39.09 mm vs 34.15–38.77 mm; p = 0.864), anterior chamber depth (ACD: 3.18 ± 0.38 mm vs 3.25 ± 0.39 mm; 95% CI: 2.78–3.58 mm vs 2.84–3.66 mm; p = 0.782), and latero-medial globe diameter (LMG: 37.02 ± 1.80 mm vs 36.98 ± 1.78 mm; 95% CI: 35.15–38.89 mm vs 35.11–38.86 mm; p = 0.970). Posterior parameters included posterior chamber depth (PCD: 15.86 ± 0.73 mm vs 16.03 ± 0.72 mm; 95% CI: 15.10–16.63 mm vs 15.27–16.79 mm; p = 0.700), central lens diameter (CDL: 9.32 ± 0.44 mm vs 9.94 ± 0.52 mm; 95% CI: 8.86–9.78 mm vs 9.40–10.48 mm; p = 0.051), latero-medial lens diameter (LML: 15.67 ± 0.56 mm vs 15.79 ± 0.55 mm; 95% CI: 15.08–16.25 mm vs 15.21–16.37 mm; p = 0.713), and posterior wall thickness (PWT: 2.03 ± 0.21 mm vs 1.98 ± 0.21 mm; 95% CI: 1.80–2.25 mm vs 1.75–2.20 mm; p = 0.672) (Table 3). The central lens diameter approached conventional significance (p= 0.051). Coefficients of variation (CV%) for the measured parameters ranged from 3.5% for LML to 12% for ACD and PWT. Confidence intervals were recalculated to ensure consistency with the reported means and standard deviations; for example, the left eye MAL 95% CI is 34.15–38.77 mm, correcting a previously misreported lower bound of 33.07 mm. Overall, no statistically significant interocular differences were detected for any measured parameter (Table 3).

DISCUSSION

The ocular morphology of the donkey (*Equus asinus*) exhibits distinct anatomical characteristics, which are reflected in our CT-based measurements and can be contextualized using previously reported literature. Although our study did not directly examine other species, literature indicates that the horse (*Equus caballus*) has a relatively flattened anterior–posterior globe (Schwedes and Wentura, 2012), whereas the donkey eyeball is generally smaller and more spheroidal, consistent with the roughly spheroidal shape observed in our CT reconstructions. Our measured globe dimensions, including maximum axial length (MAL: 36.78 ± 3.23 mm) and latero-medial diameter (LMG: 37.02 ± 1.80 mm), align closely with previously reported ultrasonographic ranges in donkeys (Laus *et al*., 2013; Salavati *et al*., 2017; Wafy *et al*., 2021), validating the use of CT for high-resolution anatomical assessment.

Histomorphologically, the donkey eye features a transparent, broad, circular cornea supported by a robust lens (Attaai *et al*., 2022), consistent with our finding of relatively uniform lens diameters, and a narrow, horizontal pupil (Zayed *et al*., 2012) likely contributing to the panoramic visual field typical of prey species. Literature notes that the tapetum lucidum is absent in primates (Dyce *et al*., 2010) but more prominent in donkeys than in some other livestock species, such as sheep, which possess a broad tapetum fibrosum (Dalga *et al*., 2022; Dyce et al., 2022; Klećkowska-Nawrot *et al*., 2023; Ollivier *et al*., 2004); our measurements of globe dimensions and chamber depths provide morphometric context for this reflective layer. The nictitating membrane (third eyelid) is supported by cartilage and covered by a conjunctival layer that may be pigmented on its anterior surface and free

margin (Dyce *et al*., 2010), complementing our assessment of anterior chamber morphology. Comparisons with horse ocular data indicate that the donkey eye is approximately 2–3 mm smaller in diameter than the horse eye (39.4 ± 2.3 mm) (Herman, 2009). Although modest, this difference is clinically meaningful, as applying equine reference values to donkeys could result in misestimation of lens size, globe dimensions, or intraocular lens calculations.

Interocular comparisons in our cohort did not reveal statistically significant differences; however, due to the small sample size and lack of prior power analysis, subtle asymmetries cannot be excluded. While the central lens diameter approached conventional significance, the study was exploratory and not powered to detect small or moderate interocular differences. Post hoc calculations indicate that with n= 8 paired observations, only large effect sizes (Cohen's d ≥ 1.0) could be reliably detected. Subtle asymmetries may therefore have gone undetected. The observed coefficients of variation (CV%) were within acceptable biological ranges, with thinner structures such as the posterior wall naturally showing higher relative variation. The posterior wall thickness (PWT) measured via CT averaged 2.03 ± 0.21 mm, providing a species-specific reference for identifying abnormal thickening in conditions such as glaucoma, ocular neoplasia, or retinal disease, thereby guiding further diagnostic evaluation or intervention (Jonas *et al*., 2014; Park *et al*., 2014). Taking together, these results highlight the importance of larger, adequately powered studies to determine whether near-significant differences, such as in central lens diameter, reflect true biological asymmetry or sampling variability.

CT-based 3D reconstructions generated from enucleated eyes under ex vivo conditions provided high-fidelity, interactive models of donkey ocular anatomy. While these models were not applied clinically, they offer valuable educational tools for visualizing orbital structures and align with ethical alternatives to animal dissection in accordance with the "3Rs" principle (Replacement, Reduction, and Refinement) (Elias *et al*., 2021; Pereira *et al*., 2017). Post-mortem changes, including loss of intraocular pressure, tissue relaxation, and dehydration, may have influenced certain measurements, and quantitative validation of the reconstructed or printed models was not performed; therefore, these models and CT-derived dimensions should be interpreted as qualitative anatomical references rather than validated clinical standards. Despite these limitations, the study provides species-specific ocular measurements that complement ultrasonographic data, highlight clinically relevant differences from horses, and demonstrate the educational potential of CT-based 3D reconstructions. Future studies incorporating *in vivo* imaging, larger sample sizes, repeatability assessments, and dimensional validation of 3D printed models are warranted to enhance measurement precision, evaluate interocular differences, and strengthen both the clinical and educational utility of donkey ocular biometry.

CONCLUSION

This study established reference values for intraocular dimensions in clinically normal donkeys using CT-scan biometry. Statistical analysis revealed that no significant interocular differences were detected in this cohort. ocular characteristics. Based on these findings, an interactive anatomical eye prototype was developed to model internal structures for surgical training. This model serves as an innovative educational tool, providing a high-fidelity alternative to cadaveric specimens in veterinary anatomy and ophthalmology.

ACKNOWLEDGEMENTS

The authors would like to express their sincere gratitude to the technical staff at the Veterinary Teaching Hospitals of the Faculty of Veterinary Medicine at Cairo University and Mansoura University for their invaluable assistance and technical support throughout the duration of this research.

NOVELTY STATEMENT

This study presents a novel integration of computed tomography (CT) - based ocular biometry and three- dimensional (3D) printing for the domestic donkey (Equus asinus), a species with limited detailed ophthalmic anatomical data. To the best of our knowledge, this is the first study to generate accurate CT- derived biometric measurements of the donkey eye alongside the development of anatomically precise 3D-printed models. This approach provides a non-invasive, reproducible method for detailed ocular assessment and offers significant value for advancing comparative anatomy, improving clinical and surgical planning and enhancing veterinary education.

AUTHOR'S CONTRIBUTION

MN, AT and YA are responsible for eye dissection, MN and YA. achieved 3D scanning and printing, MA interpreted CT scan figures. All authors contributed to the manuscript's revision and reading, as well as approved the submitted version.

Ethical approval

This study follows the ethics guidelines of the Faculty of Veterinary Medicine, Cairo University, Institutional Animal Care and Use Committee (Vet-CU-IACUC) in Egypt (ethics approval number: Vet-CU. 110520251110).

Conflict of interest statement

The authors declare that they have no known competing financial interests or personal relationships that could have appeared to influence the work reported in this paper.

REFERENCES

Attaai AH, Hussein MT, Aly KH, Abdel-Maksoud FM (2022). Morphological, immunohistochemical, and ultrastructural studies of the donkey's eye with special reference to the AFGF and ACE expression. Microsc. Microanal., 28(5): 1–14. https://doi.org/10.1017/S1431927622000666

Bagaria V, Chaudhary K (2017). A paradigm shift in surgical planning and simulation using 3D graphy: Experience of first 50 surgeries done using 3D-printed biomodels. Injury, 48(11): 2501–2508. https://doi.org/10.1016/j.injury.2017.08.058

Bloom W, Fawcett DW (1970). A textbook of histology. 10th ed. W.B. Saunders, Philadelphia.

Burden FA, Bell N (2019). Donkey nutrition and malnutrition. Vet. Clin. North Am. Equine Pract., 35(3): 469–479. https://doi.org/10.1016/j.cveq.2019.08.004

Carastro SM (2004). Equine ocular anatomy and ophthalmic examination. Vet. Clin. North Am. Equine Pract., 20(2): 285–299. https://doi.org/10.1016/j.cveq.2004.04.013

Dalga S, Aksu SI, Aslan K, Deprem T, Uğran R (2022). Anatomical and histological structures of eye and lacrimal gland in Norduz and Morkaraman sheep. Turk. J. Vet. Anim. Sci., 46(2): 336–346. https://doi.org/10.55730/1300-0128.4181

Davson H (1963). The eye. Academic Press, London.

Dyce KM, Sack WO, Wensing CJG (2010). Textbook of veterinary anatomy. 4th ed. Saunders, St. Louis.

Dyce, K. M., Sack, W. O., and Wensing, C. J. G. (2022). textbook of veterinary anatomy (6th ed.). Elsevier.

Elias NS, Pereira HCS, Neto AFL, da Silveira E, dos Santos AC, de Assis Neto AC (2021). Bioprinting of 3D anatomical models of flat and long thoracic limb bones of domestic cats (Felis catus Linnaeus, 1758). Braz. J. Vet. Med., 43(1): e106020. https://doi.org/10.29374/2527-2179.bjvm106020

Finkelstein M, Legmann A, Rubin PA (1997). Projectile metallic foreign bodies in the orbit: A retrospective study of epidemiological factors, management, and outcomes. Ophthalmology, 104(1): 96–103. https://doi.org/10.1016/S0161-6420(97)30355-8

Gelatt KN (2013). Veterinary ophthalmology. 5th ed. Blackwell Publishing, Ames. https://doi.org/10.1002/9781118910337

Grove AS Jr (1982). Computed tomography in the management of orbital trauma. Ophthalmology, 89(5): 433–440. https://doi.org/10.1016/S0161-6420(82)34770-3

Herman C (2009). The anatomical differences between the donkey and the horse. In: Matthews NS, Taylor TS (Eds.), Veterinary care of donkeys. International Veterinary Information Service (IVIS), Ithaca, NY, USA.

International Committee on Veterinary Gross Anatomical Nomenclature (ICVGAN) (2017). Nomina Anatomica Veterinaria. 6th ed. Editorial Committee, Hannover, Germany.

Jonas JB, Holbach L, Panda-Jonas S (2014). Bruch's membrane thickness in high myopia. Acta Ophthalmol., 92(6): e470–e474. https://doi.org/10.1111/aos.12372

Klećkowska-Nawrot J, Goździewska-Harłajczuk K, Kupczyńska M, Kaleta-Kuratewicz K, Kuropka P, Barszcz K (2023). Anatomical, histological and histochemical observations of the eyelids and orbital glands in the lowland tapir (Tapirus terrestris Linnaeus, 1785). Animals, 13(13): 2081. https://doi.org/10.3390/ani13132081

Lakits A, Prokesch R, Scholda C, Bankier A (1999). Orbital helical computed tomography in the diagnosis and management of eye trauma. Ophthalmology, 106(12): 2330–2335. https://doi.org/10.1016/S0161-6420(99)90536-5

Laus F, Paggi E, Faillace V, Marchegiani A, Spaziante D, Cerquetella M (2013). Ultrasonographic biometry and relationship with gender, age and weight in healthy donkeys. J. Anim. Vet. Adv., 12(7): 803–806.

Laus F, Paggi E, Marchegiani A, Cerquetella M, Spaziante D, Faillace V (2014). Ultrasonographic biometry of the eyes of healthy adult donkeys. Vet. Rec., 174(13): 326. https://doi.org/10.1136/vr.101436

Laus, F., Spaterna, A., Faillace, V., Paggi, E., Cerquetella, M., Tesei, B., Morganti, G., Laus, M. M. (2024). Surgical management of ocular diseases in donkeys (Equus asinus): Retrospective clinical study. Frontiers in Veterinary Science, 11, 1379151.

Mendoza FJ, Toribio RE, Perez-Ecija A (2018). Donkey internal medicine Part II: Cardiovascular, respiratory, neurologic, urinary, ophthalmic, dermatology, and musculoskeletal disorders. J. Equine Vet. Sci., 65: 86–97. https://doi.org/10.1016/j.jevs.2018.02.025

Misk N (1990). Ocular diseases in donkeys. Equine Pract., 12(1): 20–27.

Monti G, Bertino E, Muratore MC, Coscia A, Cresi F, Silvestro L (2007). Efficacy of donkey's milk in treating highly problematic cow's milk allergic children: An *in vivo* and *in vitro* study. Pediatr. Allergy Immunol., 18(3): 258–264. https://doi.org/10.1111/j.1399-3038.2007.00521.x

Ollivier FJ, Samuelson DA, Brooks DE, Lewis PA, Kallberg ME, Komáromy AM (2004). Comparative morphology of the tapetum lucidum (among selected species). Vet. Ophthalmol., 7(1): 11–22. https://doi.org/10.1111/j.1463-5224.2004.00318.x

Park HY, Shin HY, Park CK (2014). Imaging the posterior segment of the eye using swept-source optical coherence tomography in myopic glaucoma eyes: Comparison with enhanced-depth imaging. Am. J. Ophthalmol., 157(3): 550–557. https://doi.org/10.1016/j.ajo.2013.11.008

Pereira G, Dieguez J, Salgirli Demirbaş Y, Menache A (2017). Alternatives to animal use in veterinary education: A growing debate. Ankara Univ. Vet. Fak Derg., 64(1): 1–7.

Salavati S, Karimi S, Ahrarikhafi M (2017). Ocular ultrasonographic features in Iranian native donkey. Iran J. Vet. Surg., 11(1) : 15–19.

Salimei E, Fantuz F (2012). Equid milk for human consumption. Int. Dairy J., 24(2): 130–142. https://doi.org/10.1016/j.idairyj.2011.11.008

Samuelson DA (1999). Textbook of veterinary ophthalmology. 4th ed. Saunders, St. Louis.

Schaller O, Constantinescu GM (2007). Illustrated veterinary anatomical nomenclature. 2nd ed. Georg Thieme Verlag, Stuttgart, Germany. https://doi.org/10.1024/0036-7281.149.9.417c

Schwedes C, Wentura D (2012). The revealing glance: Eye gaze behavior to concealed information. Mem. Cogn., 40(4): 642–651. https://doi.org/10.3758/s13421-011-0173-1

Singh NK, Sahu SK (2023). Rho-kinase inhibitors: Role in

corneal endothelial disorders. Semin Ophthalmol., 38(1): 9–14. https://doi.org/10.1080/08820538.2022.2112698

Singh R, Shitiz K, Singh A (2017). Chitin and Chitosan: Biopolymers for wound management. Int. Wound J., 14(6): 1276–1289. https://doi.org/10.1111/iwj.12797

Wafy MN, Hassan EA, Abo El-Maaty AM, Abu-Seida AM (2021). B-scan biometry and color Doppler ultrasound imaging of the eye in clinically normal donkeys (*Equus asinus*): Effect of laterality, maturity and gender. J. Equine Vet. Sci., 101: 103419. https://doi.org/10.1016/j.jevs.2021.103419

Zayed AE, Aly K, Ibrahim IA, Kotb AM (2012). Comparative morphology of the iris of donkey (*Equus asinus*) and buffalo (*Bos bubalis*). J. Vet. Anat., 5(2): 75–90. https://doi.org/10.21608/jva.2012.44885